

Densification and Crystallisation Behaviour of Barium Magnesium Aluminosilicate Glass Powder Compacts

K. Lambrinou,^a O. van der Biest,^a A. R. Boccaccini^{*b} & D. M. R. Taplin^{*c}

^aDepartment of Metallurgy and Materials Engineering, Katholieke Universiteit Leuven, B-3001 Heverlee, Belgium

^bSchool of Metallurgy and Materials, University of Birmingham, Birmingham B15 2TT, UK

^cUniversity of North London, London N7 8DB, UK

(Received 15 November 1995; revised version received 25 January 1996; accepted 30 January 1996)

Abstract

The densification and crystallisation of barium magnesium aluminosilicate (BMAS) glass powder has been investigated. The aim of the study was to draw conclusions of value for the optimisation of the processing parameters for BMAS matrix ceramic composites. Pressureless sintering and hot-pressing techniques were investigated. The pressureless densification behaviour of cold-uniaxially pressed compacts was determined at isothermal and constant heating rate conditions using a high temperature microscope. The samples could be densified isothermally to full density at 930°C prior to the onset of crystallisation. For compacts sintered at constant heating rates between 800 and 1100°C, it was found that the simultaneous occurrence of crystallisation and densification strongly depends on the heating rate. Using hot-pressing (pressure = 20 MPa) results in full densification in the amorphous state after 1 hour at 925°C. X-ray diffraction analysis was used to characterise the crystallinity of pressureless sintered and hot-pressed samples that were fabricated at temperatures between 850° and 1300°C. The crystallisation behaviour did not change, in qualitative terms, with the pressure applied during hot-pressing. Combination of the densification and crystallisation results demonstrated that the BMAS glass can be densified completely at relatively low temperatures (930°C) in the glassy state. The material can be subsequently crystallised at higher temperatures (between 1100 and 1300°C) yielding a high-temperature-resistant microstructure consisting of Ba-osumilite, celsian and cordierite. Copyright © 1996 Elsevier Science Ltd

^{*}Also with: Department of Environmental Sciences, University of Plymouth PL4 8AA, UK

1 Introduction

Densification prior to crystallisation (the glass-ceramic route) is particularly important for forming high-density composites. Many experimental studies have demonstrated that glass (amorphous) matrices are easier to densify around the rigid inclusions used as reinforcement phase (such as particulates, chopped fibres, whiskers, platelets and continuous fibre tows or mats) compared with polycrystalline matrices.¹⁻⁵ At an equivalent inclusion content, glass matrices have been shown to exhibit a much higher sinterability compared to crystalline matrices,² and therefore the beneficial sintering characteristics of glass can be conveniently exploited. After the densification step, however, it is necessary to control the nucleation and growth of the crystalline phase to obtain the required crystalline microstructure for structural or high-temperature applications. If the onset of crystallisation occurs before the glass has reached full density, further densification will be impeded by crystallisation due to the increase in viscosity caused by the crystalline phase.^{1,6-8} In this context, an understanding of the interaction between densification and crystallisation of a given glass during sintering is essential for optimisation of the processing parameters which lead to the objective of obtaining a fully dense material before the onset of crystallisation occurs. Renewed interest has arisen, therefore, in studies of the sintering and crystallisation behaviour of glasses with compositions suitable for post-sintering crystallisation, which are candidate matrices for composites for high-temperature applications. While for dispersion-reinforced composites a pressureless sintering route may be applied to obtain dense products,^{1-5,9} the use of continuous reinforcement, such as long

fibres or fibre mats, requires hot-pressing to achieve complete densification.¹⁰ Thus, the interaction of densification and crystallisation in glass-ceramics must be investigated for both techniques, i.e. pressureless sintering and hot-pressing, for a complete assessment of the material as a candidate composite matrix.

The present study involves a comprehensive investigation of the densification and crystallisation behaviour of a barium magnesium aluminosilicate (BMAS) glass. The investigations were directed to gain useful information on the material's behaviour, allowing for the optimisation of processing parameters, rather than to perform a detailed study of the physics and kinetics of the processes involved. A similar BMAS material has been investigated in commercially available glass-ceramic matrix composites reinforced with SiC (Tyranno) fibres.^{11,12} These are thought to be useful for structural applications at high temperature (up to $\sim 1100^\circ\text{C}$).^{11,12} Another group has studied extensively the mechanical behaviour of SiC (Nicalon) fibres-reinforced composites with similar BMAS glass-ceramic matrices.^{13,14} Little is known, however, about the matrix densification and crystallisation behaviour during the processing of these materials.

2 Experimental Procedure

A commercial BMAS glass powder (provided by AEA Technology, Harwell) was used in this work. The theoretical density of the glass used is 2.74 g/cm^3 , as determined in a previous work.¹⁵ Quantitative Electron Micro Probe Analysis (EMPA) and X-ray diffraction (XRD) analysis were conducted on the as-received material to determine its exact composition and crystallinity. The as-received glass cullet was milled in a planetary mill and classified to obtain two mean particle sizes, 10.5 and $6.9\text{ }\mu\text{m}$ with narrow size distributions, as measured by laser diffraction analysis (Coulter L5130). Scanning electron microscopy (SEM) was used to investigate the glass powder morphology. Milled powder was used for Differential Scanning Calorimetry (DSC) measurements at heating rates of 10°C/min . In a previous study the surface energy and the viscosity of the glass (at 930°C) were determined to be $\gamma = 0.440\text{ N/m}$ and $\eta = 8.1 \times 10^7\text{ Pa s}$ respectively.¹⁶

The experimental technique chosen for studying the pressureless densification behaviour is high-temperature microscopy, because it provides a number of advantages over dilatometry, as reviewed recently.¹⁷ The most relevant advantage, in relation to the sintering of glass compacts, is the possibility of measuring both axial and radial shrinkages

without exertion of external loads that could significantly affect viscous flow behaviour. Thus, 'true' pressureless sintering experiments can be conducted.¹⁷ A complete description of the technique has been given elsewhere:^{4,15,17} only relevant details will be presented here. Cylindrical compacts (5 mm in diameter by 5 mm) were used, which were formed by uniaxial compression of the $10\text{-}\mu\text{m}$ powder in a die without using a binder. Green densities of 0.51 ± 0.02 of the theoretical were obtained using pressures of 250 MPa . For the isothermal experiments the furnace of the heating microscope was first heated to the sintering temperature (which after trial and error experiments was determined to be $T = 930^\circ\text{C}$) and subsequently the compacts were inserted quickly, in order to provide isothermal conditions for the whole stage of sintering. For the constant heating rate experiments the specimens were first heated to 800°C in about 1 hour with no glass sintering (shrinkage) observed up to this temperature. Then the samples were heated at a constant heating rate to a final temperature of 1100°C . Two heating rates, 15°C/min and 1°C/min , were used and two specimens were used for each heating rate and the results averaged. For both sets of experiments photographs of the samples were taken to record the lengths and diameters of the samples at pre-determined intervals during the sintering process. In this way the axial and radial shrinkages could be calculated as explained elsewhere.¹⁵ The mass and dimensions of the pressed and sintered compacts were measured and the geometrical densities determined. The final density of the sintered pellets was also measured using Archimedes' principle. The density as a function of time and temperature during sintering was determined from the green density and the measured axial and radial shrinkages, as shown below. Polished cross-sections of the sintered cylinders were prepared and the microstructures were observed by SEM. The crystalline composition of selected sintered samples was investigated by XRD analysis of polished surfaces.

The densification and crystallisation of the BMAS glass were also studied under hot-pressing conditions, since this is the technique relevant for manufacturing continuous-fibre-reinforced composites. The powder milled to an average particle size of $6.9\text{ }\mu\text{m}$ was used for these experiments. This is the optimum particle size for fabricating composites via a slurry infiltration technique, as determined elsewhere.¹⁸ Hot-pressing of 30-mm diameter specimens was performed, using a KCE model facility, in vacuum at different temperatures, pressures and holding times. Three pressures (5.7 , 12 and 20 MPa) were used. On the basis of the constant-heating-

rate and pressureless sintering experiments, a very quick heating rate was chosen to avoid crystallisation occurring prior to complete densification. The heating rates in all experiments were fixed at 100°C/min. A typical hot-pressing cycle involved heating up at 100°C/min to the holding temperature, which was varied between 850 and 1000°C, followed by a dwell time, which was varied between 2.5 and 60 min and then cooling down in the hot-press. In all cases the pressure started to be applied at 850°C and was maintained until the beginning of cooling. In another set of experiments, involving temperatures $\geq 1000^\circ\text{C}$, the sample was heated up to 900°C, maintained at this temperature for 15 min, subsequently heated up to a higher temperature, which was varied between 1000 and 1300°C, for given holding times, and finally cooled down. Here again the pressure started to be applied at 850°C and was maintained until the beginning of cooling. Post-fabrication pressureless heat treatment of samples that had been fabricated by hot-pressing at 950°C for 60 min with 12 MPa applied pressure was also carried out. As-hot-pressed and heat-treated samples were characterised by XRD analysis of polished surfaces. Selected samples were polished and prepared for SEM observation.

3 Results and Discussion

3.1 Material characterisation

The XRD pattern of the as-received glass powder is shown in Fig. 1, indicating that the material is amorphous in the range of detectability of XRD. The chemical composition of the as-received material, as determined by EMPA analysis is shown in Table 1. Figure 2 shows a SEM micrograph of the glass powder after milling to a mean particle size of 10 μm . The nonspherical shape of the particles, an important variable affecting the sintering behaviour of this glass as shown elsewhere,¹⁶ is evident. The DSC curve, shown in Fig. 3, indicates that the softening point of the glass is 850°C, its crystallisation takes place between 1080 and

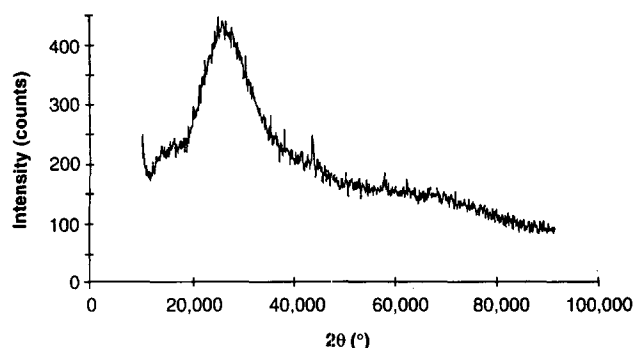


Fig. 1. XRD pattern of the as-received BMAS glass powder, showing its amorphous character.

Table 1. Chemical composition of as-received BMAS glass

Oxide	Content (wt%)
BaO	13.9 \pm 0.5
Al ₂ O ₃	27.7 \pm 0.5
SiO ₂	52.0 \pm 1.0
MgO	6.4 \pm 0.2

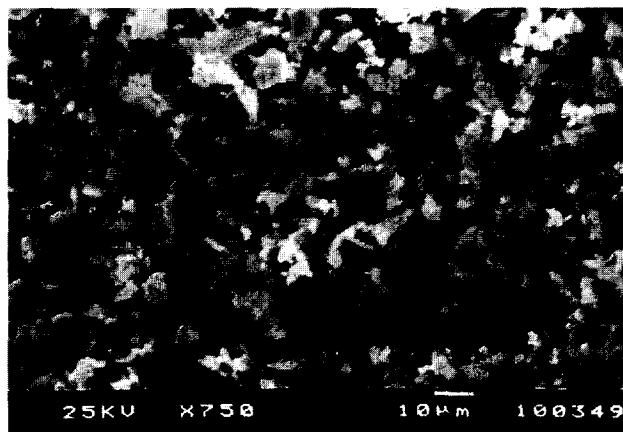


Fig. 2. Scanning electron micrograph of the BMAS glass powder investigated after milling to a mean particle size of 10 μm .

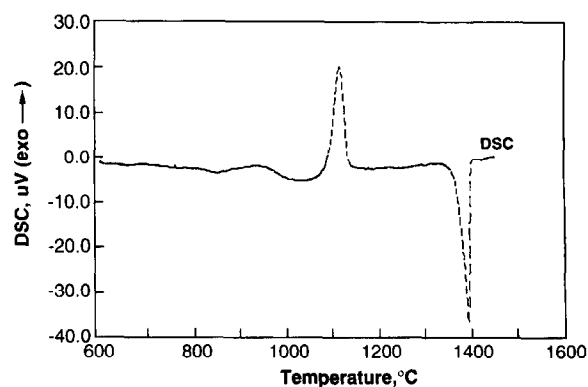


Fig. 3. DSC curve of BMAS powder milled to a mean particle size of 5.8 μm showing the exothermic crystallisation peak between 1080 and 1140°C.

1140°C with the peak crystallisation temperature at $\approx 1120^\circ\text{C}$, while the melting point lies at $\approx 1400^\circ\text{C}$. These results supplied a preliminary guideline according to which the further densification and crystallisation experiments were designed.

3.2 Pressureless densification behaviour

Comprehensive studies of the sintering behaviour of BMAS powder compacts have been conducted recently^{15,16} including a comparison of experimental values with theoretical models for viscous sintering, the consideration of shrinkage anisotropy effects and the assessment of densification and creep rates. Therefore, only a summary of the relevant results pertinent for the purposes of this paper will be presented in the following sections.

3.2.1 Sintered density

From the experimental data for the axial and radial shrinkages during sintering supplied by the heating microscopy measurements, the density (ρ) at any time (for the isothermal sintering experiments) or temperature (for the constant-heating-rate experiments) can be found using the following equation.^{4,17}

$$\rho = \frac{\rho_0}{(1 - \Delta R/R_0)^2 (1 - \Delta H/H_0)} \quad (1)$$

where $\Delta R = R_0 - R$, $\Delta H = H_0 - H$ and ρ_0 represents the green density. R_0 and H_0 are the initial radius and length, respectively, and R and H are the instantaneous radius and length, respectively, of the sample.

Figures 4(a) and (b) show the densification curves for samples sintered isothermally at 930°C and at two different constant heating rates, 15 and 1°C/min, respectively. The density values were calculated using eqn (1), the data for radial and axial shrinkage, and the green densities. The data shown are averages of two runs under the same conditions

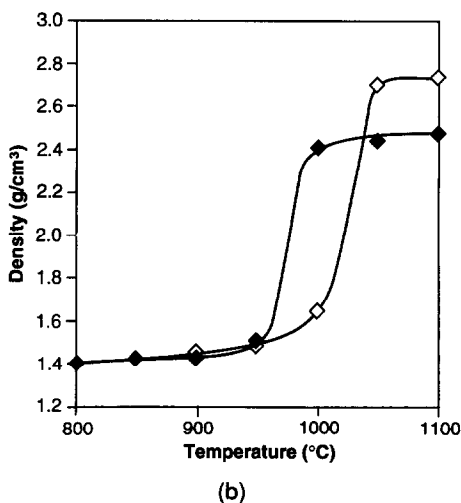
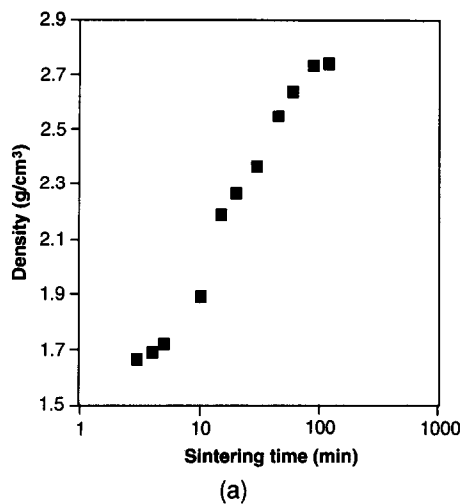


Fig. 4. Densification behaviour of BMAS glass powder compacts pressureless sintered: (a) isothermally at 930°C and (b) under constant heating rate conditions of (\diamond) 15°C/min and (\blacklozenge) 1°C/min.

and have a maximum relative error of 4%. The final densities calculated from eqn (1) were in good agreement with the values determined using Archimedes' principle. Interesting conclusions about the pressureless densification behaviour of BMAS glass powder compacts can be drawn from Fig. 4. It is shown, for example, that a fully densified body ($\rho = 2.74 \text{ g/cm}^3$) can be obtained after two hours of isothermal sintering at 930°C, a result which supports the technological approach of producing dense glass-ceramics in the BMAS system via a simple pressureless powder technological route. That the densification of BMAS powder at this temperature takes place via a viscous flow mechanism was confirmed in a previous study¹⁶ by comparing the experimental results with the prediction of a theoretical model for viscous flow sintering.¹⁹

Figure 4(b) demonstrates qualitatively the influence of heating rates on the interaction between densification and crystallisation. It is observed that for both heating rates the densification curves reach a plateau. However, the reason for this is different for each heating rate. For the faster heating rate (15°C/min), the plateau is reached because the sample is nearly fully densified at $\approx 1050^\circ\text{C}$ with a relative density $\approx 98\%$ of the theoretical. For the lower heating rate (1°C/min) there must be another reason for the abrupt change in the slope of the densification curve at a lower temperature (1000°C), since the density is only $\approx 89\%$ of the theoretical. This behaviour can be attributed to the onset of crystallisation at this temperature, as shown in a separate study,²⁰ in which the shear strains for both heating rates were calculated. The curve for the lower heating rate showed a typical sigmoidal behaviour with the shear strain first increasing with temperature as the viscosity of the glass decreases. An abrupt change in slope occurred near 1000°C, however, indicating that the material became suddenly more viscous, i.e. it began to crystallise. This can be directly related to the change of slope in the densification curve at approximately the same temperature, as shown in Fig. 4(b). These results are also in qualitative agreement with the DSC measurements (Fig. 3), that showed the onset of crystallisation at $\approx 1080^\circ\text{C}$. This temperature is slightly higher than that indicated by the densification curve of the 1°C/min sample (Fig. 4(b)), which is probably because the DSC measurements were carried out at a higher heating rate (10°C/min). Thus increasing heating rate delays the onset of crystallisation, as found by others.^{6,7} Observation of the microstructure by SEM and the results of XRD analysis confirm that, for the compacts heated at the lower heating rate, crystallisation took place before completion of the densification process, as shown next.

3.2.2 Microstructural observation

Figures 5 and 6 show SEM micrographs of samples sintered isothermally for two hours at 930°C and at 1°C/min up to 1100°C, respectively. The material sintered at 930°C remained amorphous, at least in the detectability limit of XRD, and it is fully dense with only some isolated pores visible. On the contrary, using a low heating rate (1°C/min) has resulted in the early (partial) crystallisa-

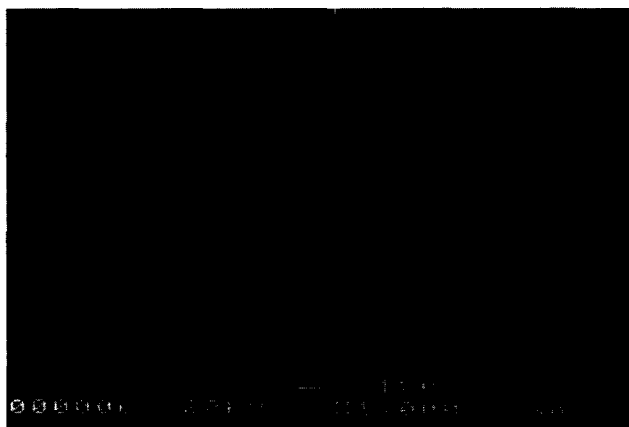


Fig. 5. Scanning electron micrograph of a polished section of a compact pressureless sintered for two hours at 930°C. Complete densification has been achieved without crystallisation.

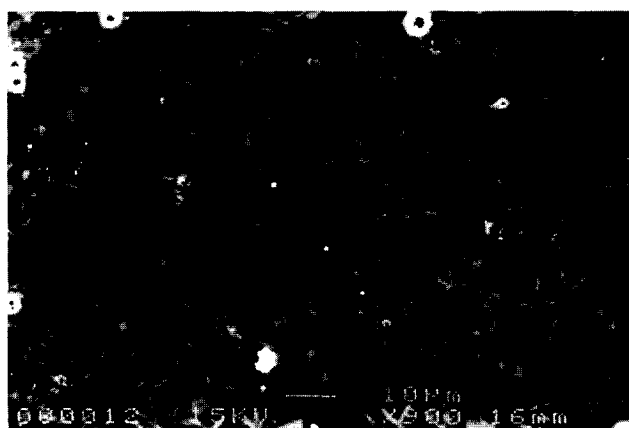


Fig. 6. Scanning electron micrograph of a polished section of a compact pressureless sintered at 1°C/min to 1100°C. Partial crystallisation and residual porosity are evident.

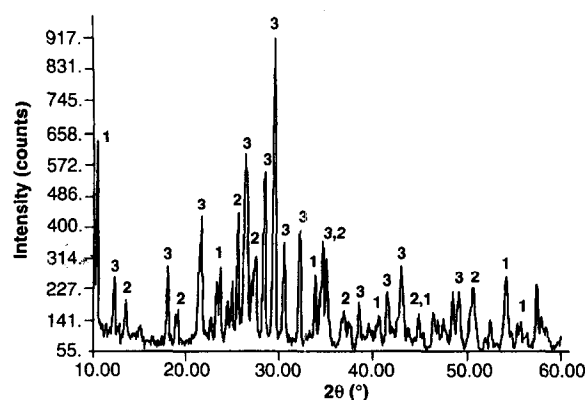


Fig. 7. XRD pattern of the polished surface of a sample sintered under the conditions given in Fig. 6 showing the appearance of: 1 = cordierite, 2 = celsian, 3 = Ba-osumilite.

tion of the material and the lack of complete densification. The XRD pattern of this sample is shown in Fig. 7. Celsian, Ba-osumilite and cordierite are the main crystalline phases found. This result is comparable with the crystallisation of the hot-pressed samples, as shown in the next section.

3.3 Hot-pressing technique

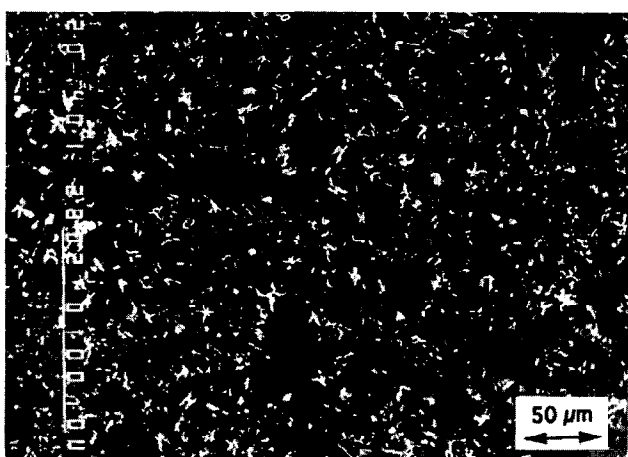
3.3.1 Densification behaviour

The results of the density measurements of the as-hot-pressed samples indicated that complete densification could not be achieved for the lowest pressure employed (5.7 MPa) and holding times shorter than 1 hour, even for temperatures up to 1000°C. Compared with the pressureless sintering experiments described above, this result shows the importance of a sufficient holding time for achieving a fully dense sample, as well as the optimisation of the heating rates. Although the extremely high heating rates employed in the hot-pressing experiments are effective in suppressing the onset of crystallisation, they may negatively affect the viscous flow behaviour of the glass, leading to the development of closed cavities, which could not be completely eliminated by mass transport via viscous flow due to the short dwell times employed (<60 min). Complete densification could be achieved, on the other hand, for samples pressed at higher pressures. Pressing for 60 min at 950°C using a pressure of 12 MPa and at 925°C using 20 MPa resulted in complete densification. Thus, as expected, when compared with the pressureless sintering experiments, application of external pressure during sintering has reduced the densification time significantly but has not modified the sintering temperature.

The relative influence of temperature and pressure on densification can be further assessed by considering the experiments at higher temperatures using the low pressure of 5.7 MPa. As mentioned above the hot-pressing experiments for which the holding temperatures were above 1000°C comprised an initial step in which the sample was held for 15 min at 900°C. Microstructural examination done on samples pressed at 5.7 MPa proved that 15 min 'soaking' time at 900°C was insufficient to densify the glass completely. This is demonstrated by Figs 8(a) and 8(b), SEM micrographs of samples hot-pressed at 1070°C for 30 min and at 1300°C for 60 min, respectively, in which considerable homogeneously distributed spherical porosity is presented. This result is a further demonstration that once crystallisation has begun the material can no longer be fully densified, even using temperatures as high as 1300°C for 60 min, Fig. 8(b), and a residual porosity remains.



(a)



(b)

Fig. 8. Scanning electron micrographs of polished sections of samples hot-pressed using 5.7 MPa for (a) 30 min at 1070°C and (b) 60 min at 1300°C. The samples were partially crystallised before densification was completed.

3.3.2 Crystallisation behaviour

Crystallised glass-ceramics produced by hot-pressing of amorphous BMAS glass under pressures of 5.7, 12 and 20 MPa contained without exception Ba-osumilite ($\text{BaMg}_2\text{Al}_3(\text{Si}_9\text{Al}_3\text{O}_{30})$ -hexagonal) as the major phase, and celcian ($\text{BaAl}_2\text{Si}_2\text{O}_8$ -monoclinic) and cordierite ($\text{Mg}_2\text{Al}_4\text{Si}_5\text{O}_{18}$ -orthorhombic) as the minor phases. These phases have been found to be the main components in commercial BMAS glass-ceramic composite products,^{11–14} being responsible for the high-temperature capability ($\approx 1100^\circ\text{C}$) of these composites. Considering the results for all hot-pressed samples it is found that the material always becomes crystalline if it is pressed at 1025°C for 20 min or more. A typical XRD diagram is shown in Fig. 9. When compared with the results for the pressureless sintered material sintered at a low heating rate (1°C/min) (Fig. 7), the results for the hot-pressed samples indicate that the application of external pressure during densification has no major effect, at least

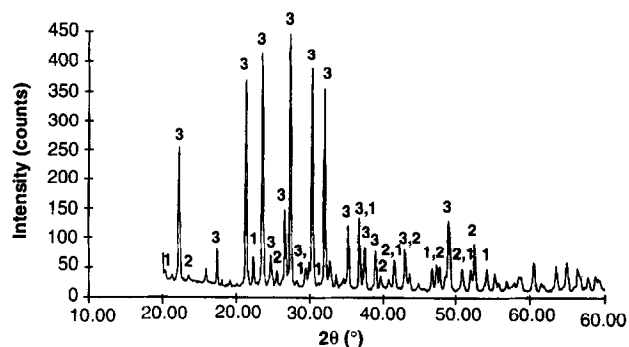


Fig. 9. Typical XRD pattern for hot-pressed samples fabricated at any pressure, showing crystallisation: 1 = cordierite, 2 = celcian, 3 = Ba-osumilite.

qualitatively, on the crystalline structure developed in BMAS glass-ceramics. A more detailed quantitative investigation of the crystallisation behaviour during hot-pressing, including crystal nucleation and growth processes and their dependence on pressure, time and temperature, is the focus of on-going studies.¹⁸ On reference to Fig. 8(a) it can be seen that the microstructure of the crystalline samples contains white dendritic crystals spread inside the bulk glassy material and some 'eutectic-like' formations. EPMA measurements on the different phases showed that the composition of the dendrites is close to the stoichiometric composition of Ba-osumilite, while the composition of the 'eutectic-like' formations varies between the compositions of Ba-osumilite and celcian. The similarity between the microstructures of the partially densified hot-pressed samples, Figs 8(a) and 8(b), and the pressureless sintered sample that was sintered at the low heating rate of 1°C/min (Fig. 6) should also be noted.

The crystallisation behaviour was also investigated by long-duration (12 h) heat-treatment of hot-pressed dense samples after they had been cooled down to room temperature. A SEM micrograph of a sample hot-pressed for 60 min at 950°C and 12 MPa is shown in Fig. 10. Although this material was amorphous under XRD analysis, the presence of a few isolated crystals with dendritic shape is evident in the micrograph. The further micrographs, Figs 11(a)–(c), are SEM micrographs showing the microstructure of dense hot-pressed samples after heat treatment for 12 h at 1070, 1120 and 1300°C, respectively. Again Ba-osumilite was the main phase found, although celcian and cordierite were also present, as revealed by EPMA. In Fig. 11(a) the different crystalline phases are indicated. The big dark grey areas correspond to Ba-osumilite crystals, while celcian and cordierite appear as forming a network (celcian being the bright phase and cordierite the black one). The crystals are surrounded by an amor-

phous 'matrix' which appears of a homogeneous grey colour. With increasing heat-treatment temperature clearly the crystallinity of the samples also increases, with fewer islands of amorphous matrix phase. The number of the big Ba-osumilite

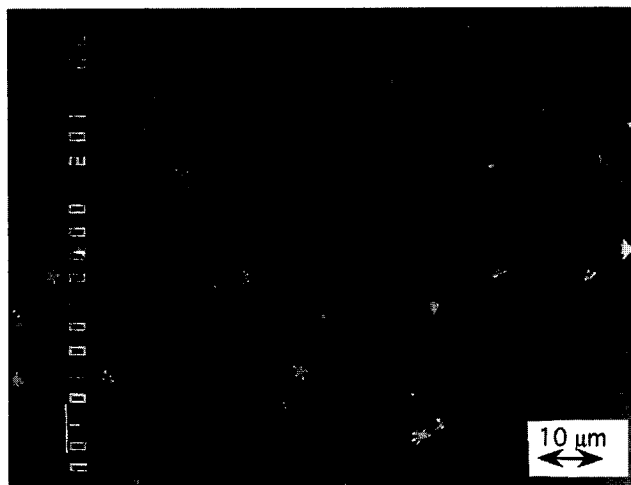
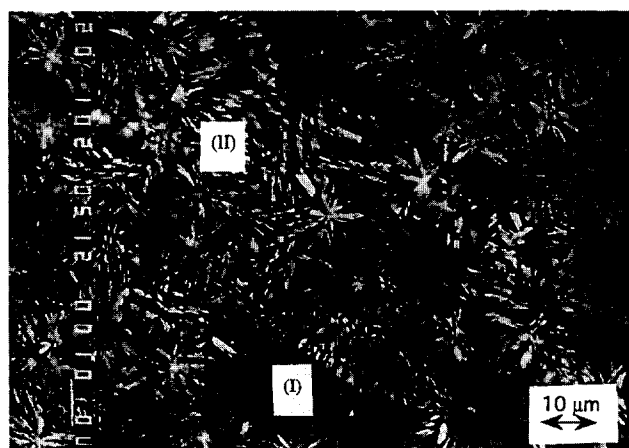


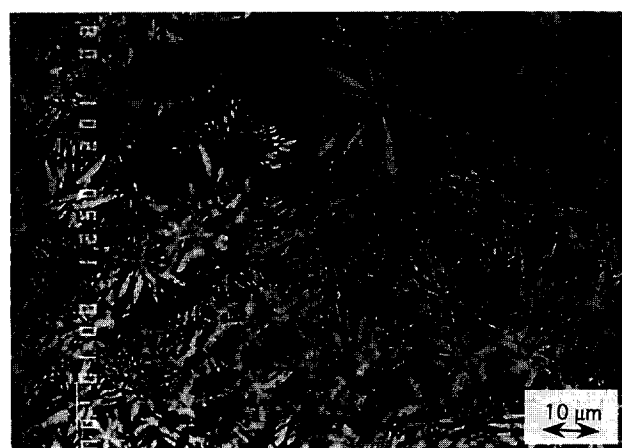
Fig. 10. Scanning electron micrographs of the polished section of a compact hot-pressed at 950°C for 60 min using 12 MPa. Complete densification has been achieved and a few dendritic crystals are distributed in the glassy matrix.

crystals decreases with higher heat-treatment temperatures, while the interconnectivity of the celsian/cordierite network increases, Figs 11(b) and (c). Long-term heat-treatment at 1300°C, therefore, seems to be sufficient for complete 'ceraming' of the material. A more detailed study of the crystallisation kinetics, however, is beyond the scope of this work, being the subject of ongoing studies.¹⁸

From the results of the XRD analyses, a Transformation-Temperature-Time (TTT) diagram, can be drawn. It approximately indicates the temperature/time 'window' for fabricating glass-ceramics from the amorphous BMAS powder by viscous flow densification in the glassy state, without crystallisation occurring. Such a diagram is shown in Fig. 12, where also the results of the pressureless sintering route have been included. Thus, the data represented in the TTT diagram can be conveniently used for designing the manufacturing route, via pressureless sintering or hot-pressing, of monolithic BMAS glass-ceramics and BMAS glass-ceramic matrix composites.



(a)



(b)



(c)

Fig. 11. Scanning electron micrographs of polished sections of samples hot-pressed under the conditions given in Fig. 10 and subsequently heat-treated for 12 h at: (a) 1070°C, (b) 1120°C and (c) 1300°C. (I) Ba-osumilite, (II) celsian/cordierite network. Crystallisation increases with heat-treatment temperature.

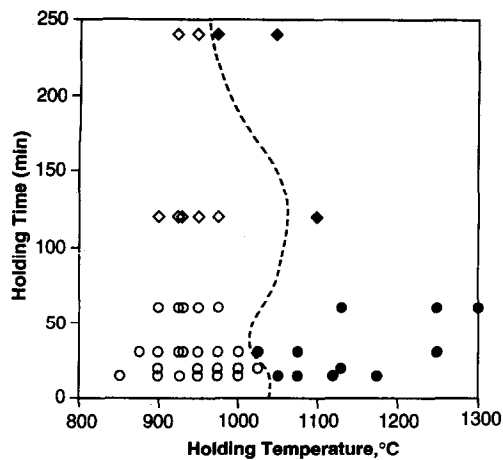


Fig. 12. TTT diagram constructed from the results of the XRD analyses for hot-pressing and pressureless sintering conditions: (◇) amorphous state, pressureless sintering, (○) amorphous state, hot-pressing, (◆) crystalline state, pressureless sintering, (●) crystalline state, hot-pressing.

4 Conclusions

A non-spherical BMAS glass powder with a composition suitable for producing glass-ceramics after a post-sintering heat-treatment was investigated in terms of densification and crystallisation behaviour. By appropriate selection of processing parameters, in pressureless sintering and hot-pressing techniques, complete densification can be achieved by viscous flow before the onset of crystallisation at relatively low temperatures (930°C). By subsequent heat-treatment at higher temperatures the desired refractory crystalline microstructure containing Ba-osumilite, celsian and cordierite is developed. These results are useful for designing the fabrication route for preparing BMAS glass-ceramics and fibre-reinforced BMAS glass-ceramic matrix composites.

Acknowledgements

The authors acknowledge the financial support of the European Commission with the provision of Brite-Euram contracts BE 4610, BRE2-CT93-3004 and BRE2 CT94 3064.

References

- Jeng, D. Y. & Rahman, M. N., Effect of rigid inclusions on the sintering of mullite synthesized by sol-gel processing. *J. Mat. Sci.*, **28** (1993) 4421–6.
- Bordia, R. K. & Raj, R., Analysis of sintering of a composite with a glass or ceramic matrix. *J. Am. Ceram. Soc.*, **69** (1986) C-55–C-57.
- Boccaccini, A. R., Sintering of glass powder compacts containing rigid inclusions. *Sci. Sint.*, **23** (1991) 151–8.
- Boccaccini, A. R., Sintering of glass matrix composites containing Al₂O₃ platelet inclusions. *J. Mat. Sci.*, **29** (1994) 4273–8.
- Rahaman, M. N. & De Jongue, L. C., Effect of rigid inclusions on the sintering of glass powder compacts. *J. Am. Ceram. Soc.*, **70** (1987) C-348–C-355.
- Panda, P. C. & Raj, R., Sintering and crystallisation of glass at constant heating rates. *J. Am. Ceram. Soc.*, **72** (1989) 1564–6.
- Rudolph, T., Weisskopf, K., Pannhorst, W. & Petzow, G., Microstructural development of a P₂O₅-modified cordierite glass-ceramic during sintering. Part 2. *Glastech. Ber.*, **64** (1991) 305–9.
- Du, Y.-J., Holland, D. & Pittson, R., Sintering and crystallisation behaviour of BaO-Al₂O₃-SiO₂ and BaO-ZnO-Al₂O₃-SiO₂ xerogel powders. *Phys. Chem. Glasses*, **34** (1993) 104–8.
- Dutton, R. E. & Rahaman, M. N., Sintering, creep and electrical conductivity of model glass-matrix composites. *J. Am. Ceram. Soc.*, **75** (1992) 2146–54.
- Prewo, K. M., Brennan, J. J. & Layden, G. K., Fibre reinforced glasses and glass-ceramics for high performance applications. *Ceram. Bull.* **65** (1986) 305–22.
- Fibre Reinforced Ceramics. Product Information.* AEA Technology Harwell, UK, 1992.
- West, G., Boccaccini, A. R. & Taplin, D. M. R., Creep and creep-fatigue behaviour of continuous fibre reinforced glass-ceramic matrix composites. *Matwiss. u. Werkstofftech.*, **26** (1995) 368–73.
- Brennan, J. J., Interfaces in BN coated fiber reinforced glass-ceramic matrix composites. *Scr. Metall. Mat.*, **31** (1994) 959–64.
- Sun, E. Y., Nutt, S. R. & Brennan, J. J., Interfacial microstructure and chemistry of SiC/BN dual-coated Nicalon-fiber-reinforced glass-ceramic matrix composites. *J. Am. Ceram. Soc.*, **77** (1994) 132–9.
- Boccaccini, A. R., Taplin, D. M. R., Trusty, P. A. & Ponton, C. B., Creep and densification during anisotropic sintering of glass powders. *J. Mat. Sci.*, **30** (1995) 5652–6.
- Boccaccini, A. R., Trusty, P. A. & Taplin, D. M. R., Anisotropic shrinkage of barium magnesium aluminosilicate glass powder compacts during sintering. *Mat. Letters*, **24** (1995) 199–205.
- Boccaccini, A. R. & Bossert, J., Using the Leitz heating microscope to study the sintering behaviour of powder compacts. *Mitt. f. Wiss. u. Tech.*, **10** (1994) 274–82.
- Lambrinou, K., PhD Thesis, KUL-Leuven, in preparation (1995).
- Exner, H. E. & Giess, E. A., A stereology-based equation for isotropic shrinkage during sintering by viscous flow. In *Proceedings of the VII World Round Table Conference on Sintering*, Herceg-Novi, Yugoslavia, Plenum Press, NY, 1990, pp. 73–83.
- Boccaccini, A. R., Stumpfe, W., Taplin, D. M. R. & Ponton, C. B., Densification and crystallisation of glass powder compacts during constant heating rate sintering. *Mat. Sci. Eng. A*, (1996) accepted.